J. Mt. Sci. (2012) 9: 879–890
DOI: 10.1007/s11629-012-2447-x

Effect of Topography and Accessibility on Vegetation Dynamic Pattern in Mountain-hill Region

QIU Bingwen[1]*, ZHONG Ming[1], ZENG Canying[1], TANG Zhenghong[2], CHEN Chongcheng[1]

[1] *Key Laboratory of Spatial Data Mining & Information Sharing of Ministry of Education, Spatial Information Research Centre of Fujian Province, Fuzhou University, Fuzhou 350002, Fujian, China*

[2] *Community and Regional Planning Program, University of Nebraska-Lincoln, Lincoln, Nebraska, USA*

**Corresponding author, e-mail: qiubingwen@fzu.edu.cn*

Abstract: Knowledge of both vegetation distribution pattern and phenology changes is very important. Their complicated relationship with elevation and accessibility were explored through a geographically weighted regression (GWR) framework in Fujian province, China. The 16-day time series of 250 m Moderate Resolution Imaging Spectroradiometer (MODIS) Enhanced Vegetation Index (EVI) dataset from 2000 to 2010 was applied. Wavelet transform method was adopted to decompose the original time series and construct the annual maximum EVI and amplitude of the annual phenological cycle (ΔEVI). Candidate explaining factors included topographic conditions, accessibility variables and proportions of primary vegetation types. Results revealed very strong positive influence from parameters of elevation and accessibility to big rivers and negative effect from accessibility to resident on both maximum EVI and phenological magnitude through ordinary linear least square (OLS) regression analysis. GWR analysis revealed that spatially, the parameters of topography and accessibility had a very complex relationship with both maximum EVI and phenology magnitude, as a result of the various combinations of environmental factors, vegetation composition and also intensive anthropogenic impact. Apart from the continuously increasing trend of phenology magnitude with increasing altitude, the influence of topography and accessibility on maximum EVI and phenological magnitude generally decreased, even from strongly positive to negative, with increasing altitude or distance. Specially, the most rapid change of correlation coefficient between them was observed within a low elevation or close distance; less variation was discovered within a certain range of medium altitude or distance and their relationship might change above this range. Non-stationary approaches are needed to better characterize the complex vegetation dynamic pattern in Mountain-hill Region.

Keywords: Vegetation phenology; Elevation gradient; Accessibility; Geographic weighted regression; Enhanced Vegetation Index; Spatial non-stationality

Received: 21 June 2012
Accepted: 8 October 2012

Introduction

Numerous research has been carried out to investigate the spatio-temporal relationship between vegetation pattern and environmental conditions, especially the correlations among vegetation pattern, elevation and climate factors (Piao et al. 2012; Nelson et al. 2007; Beatriz Martínez and Gilabert 2009; Souza et al. 2010; Ben–Ze'ev et al. 2006; Li et al. 2010; Chamaille–Jammes et al. 2006; Rowhani et al. 2011; Chang et al. 2011; Zhong et al. 2010). Related studies can be classified into two groups: one group focuses on the vegetation distribution pattern (Nelson et al. 2007; Souza et al. 2010); the other group investigates the phenology changes, such as amplitude of the annual phenological cycle, onset and offset of greenness (Iversen et al. 2009; Chang et al. 2011; Moulin et al. 1997; Atzberger and Eilers 2011; Crimmins et al. 2010; Piao et al. 2012). Less attention is drawn on both vegetation distribution pattern and its phenology.

Among them, their relationship has been typically assumed to represent biome-specific or vegetation type-specific constant. However, recent related studies have addressed that the spatially distributed environmental variables and their relationship with vegetation varies across the geographical space (Pineda Jaimes et al. 2010; Propastin 2012; Gao et al. 2012; Zhao et al. 2010; Nelson et al. 2007; G.M 2003; Propastin 2011). The spatial non-stationary relationship has great implications for exploring the influence of environmental variables on the spatio-temporal pattern of vegetation and has not been deeply explored yet.

This paper aims to evaluate the relationship between annual maximum vegetation index, amplitude of the annual phenological cycle and environmental variables, focusing on topography and accessibility, and further investigate the underlying mechanism across the space, in a moist sub-tropical rainforest of Fujian, China. The annual maximum Moderate Resolution Imaging Spectroradiometer (MODIS) EVI and amplitude of the annual phenological cycle are utilized as indicators for vegetation distribution pattern and its phenology. Their spatial relationship is investigated through the framework of geographically weighted regression based on the wavelet transform (WT) time series datasets.

1 Materials and Methods

1.1 Study area

Fujian province is located between latitude 23°32'~28°19' N and longitude 115°50'~120°43' E. It is approximately 530 km long, the widest part is approximately 480 km^2 and the total land area is 121,400 km^2. It has a middle subtropical climate in the northern mountainous and hilly areas and a south subtropical climate in the southern coastal areas. The annual mean temperature fluctuates between 17 °C-21 °C and the yearly precipitation varies between 920 mm~2,100 mm (Lu 1999). The mean elevation of Fujian is 475 m above sea level and the mean slope is around 15°. It has a very diverse relief with elevation from zero in the coastal area in the east to 2,258 m in the northwest. Using the threshold elevations of 500 m and 50 m to delineate mountains, hills and plains, the ratios of mountain is 15:3:2 (Lu 1999). The central mountain locate in the west part and middle part, hindering the cold air from inland, to the west is the Wuyi and Shaling Mountain, in the middle is the Jiufeng and Danyun mountain. The plain situated in the downstream of several big rivers, namely Minjiang River, JiulongJiang River, Tingjiang River and Jinjiang River. Forests cover 68.7% of the land area. Coniferous forest, hardwood forest, and bamboo forest represent 66.8%, 32.2% and 13.5% of the forested area respectively (Gao 2004). Cultivated land covers 10.82% of the land area. Urban areas cover 4.47% of the land area and are mostly located below 80m elevation (Fujian 2010).

1.2 Maximum EVI and phenological magnitude based WT

This study used a 16-day time series of 250 m MODIS surface reflectance data (MOD09Q1), acquired from 2000 to 2010. The MODIS land data products incorporate enhanced atmospheric correction, cloud detection, improved georeferencing and enhanced ability to monitor vegetation (Justice et al. 1998; Pagano and Durham 1993). The Enhanced Vegetation Index (EVI) product of MODIS is designed to provide consistent, spatial and temporal comparisons of global vegetation conditions in finer details than the NDVI product of NOAA VHRR (Justice et al. 1998). NDVI could be saturated easily and exhibits very high sensitivity to canopy background variations (Huete et al. 2002). EVI produces a vegetation signal with improved sensitivity in high biomass regions and with improved vegetation monitoring through the reduction of soil and atmospheric influences (Waring et al. 2006). The map projection was converted to Universal Transverse Mercator using ENVI image processing software.

A smoothing method is required to maintain the temporal details by eliminating unusually high or low EVI values. Wavelet transform based smoothing method is applied for this purpose. The wavelet transform (WT) method is applied to 250 m MODIS EVI dataset from 2000 to 2010 to decompose the original 16-day time series into details (D) and approximation (A) series at different levels (Abry 1997). In the first level of the decomposition, the original signal is decomposed into the approximation and detailed component: $f(t) = A_1 + D_1$. In the next step, the approximation A_1 is further split as $A_1 = A_2 + D_2$, and so on. The approximation component for level 5, A5, provides information about the inter-annual variability over the considered stage, since the semi-period for level 5 is 357 days. Two parameters representing maximum level of EVI and magnitude of phenological cycle can be derived from the above series. The $EVI_{\max}$, representing the maximum level of EVI , is defined as ninety percentile of the sum of mean inter-annual and intra-annual variability: $EVI_{\max} = P_{90}(\overline{A_5 + V})$, where $V = \sum_{j=2}^{5} D_j$, which refers to the sum of the detail components up to level five and can be considered as the total intra-annual variability. Another parameter, ΔEVI indicating the amplitude of the annual phenological cycle, is calculated as the range of percentiles 10% and 90% for the intra-annual variability: $\Delta NDVI = R_{10,90}(V)$. More details on maximum EVI and phenological magnitude based WT can be found in. reports by Martínez and Gilabert (2009).

The spatial distributions of $EVI_{\max}$ and ΔEVI over the study area during 2000-2010 were provided in Figure 1. For $EVI_{\max}$, very great values were examined in a small portion of the southwestern and northeastern region, with relatively low values in the coastal areas. Considerably large ΔEVI values were observed in the western portion and several islands in the coastal areas, as opposed to lower ΔEVI values examined in the southeastern portion.

1.3 Candidate explanatory variables

The diversities of environmental and hereditary conditions are suspected to cause variability of vegetation distribution and phenological cycles. As many of the direct determinants are difficult or expensive to access (Wang et al. 2010), the physical and human geographical proxies of vegetation dynamic determinant which are easy to collect and implemented in ARCGIS were selected. Numerous studies confirmed that topographic variables, accessibility and vegetation type played an important role in the vegetation dynamic process (Liang et al. 2012; Ogden and Powell 1979; Piao et al. 2006). A detailed description of candidate explanatory variables utilized in this paper is given in Table 1. The DEM data were obtained from the USGS 1-arcsecond archive (ftp://edcsgs9.cr.usgs.gov/pub/data/srtm/United _States_1-arcsec/1arcsec/). Topographic variables, such as slope and aspect, were calculated from DEM dataset using ARCGIS software. Since aspect is cyclic variable, transformation was used to derive a continuous gradient as 100 in the south and 0 in the north. The original spatial resolution of the topographic datasets is 30 m. We resampled the topographic datasets to 250 m in accord with MODIS EVI dataset.

Other datasets used for this study consists of spatial explicit land use data and forest type data.

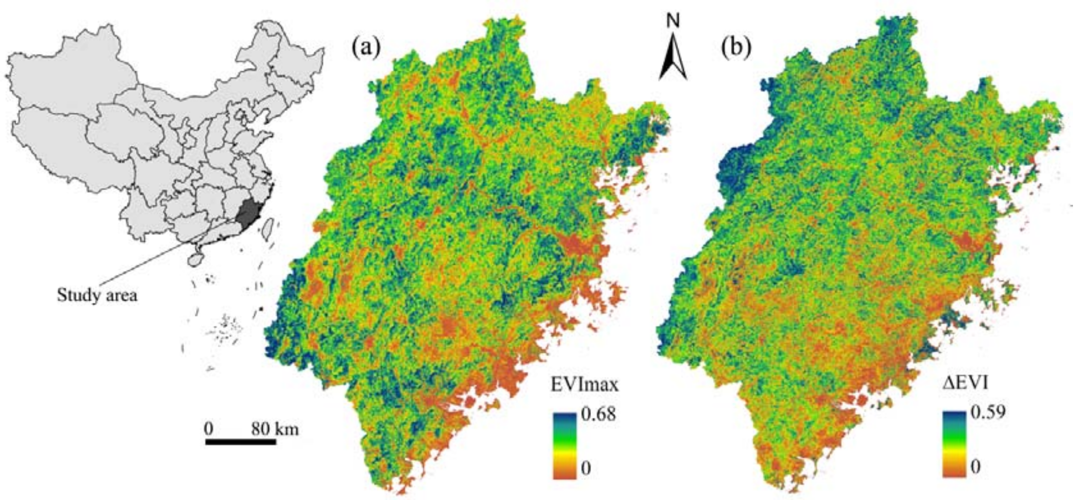

Figure 1 Location of study area and EVI dataset ((a): $EVI_{\max}$ (b): ΔEVI)

Table 1 Variables used in standard regression analysis

Variables	Explanation	unit
Slope	slope	o
Elevation	elevation	m
Aspect	Percentage areas with south aspect(-cos(aspect))	%
Lake	Distance to nearest lake(reservoir) or sub-river	m
River	Distance to nearest big river	m
Road	Distance to nearest road	m
Resident	Distance to nearest resident	m
Conifer	Percentage areas with coniferous forest	%
Hardwood	Percentage areas with hardwood forest	%

The 1:250,000 land use distribution maps are collected from the Fujian Surveying and Mapping Bureau. The 1:50,000 forest cover type data is gathered from the Fujian Forest Bureau. The accessibility variables include distance to nearest roads, residents, lakes (reservoir) or sub-rivers and big rivers. The accessibility variables were calculated through a standard distance operation in ESRI software ARCGIS 9.3. Variables of primary vegetation types, i.e. the percentage of coniferous forest and hardwood forest, were also considered. The spatial distribution maps of three key candidate variables (elevation, distance to nearest big river or resident area) were provided in Figure 2.

1.4 Geographic weighted regression analysis

Geographically weighted regression is a local regression technique that significantly improves common regression dealing with geospatial process. The global regression method assumes a constant (stationary) relationship between spatial variables over the whole study area. The GWR takes the spatial locations of samples into consideration, permitting the estimated parameters to vary locally, thus better reflecting the spatially varying relationships between the dependent and independent variables (Fotheringham et al. 2002). A GWR model can be written as.

$$y_i = \beta_0(\mu_i, \nu_i) + \sum_k \beta_k(\mu_i, \nu_i)x_{ik} + \varepsilon_i$$

where (u_i, v_i) denotes the coordinates of the ith location, and β_0 (μ_i, v_i) and β_k (μ_i, v_i) are the estimated parameters for the ith location, whose values vary with the location. For GWR, the parameters can be estimated using a weighting function (Fotheringham et al. 2002):

$$\beta(\mu,\nu) = (X^T W(\mu, \nu) X)^{-1} X^T W(\mu, \nu) y$$

where W (μ_i, v_i) are the weights which are chosen so that those observations near the point under study have more influence on the results than those farther away. In this study, we used the following Gaussian weighting kernel function form:

$$W(\mu_i, \nu_i) = \exp\left(\frac{d_{ij}^{\ 2}}{b^2}\right)$$

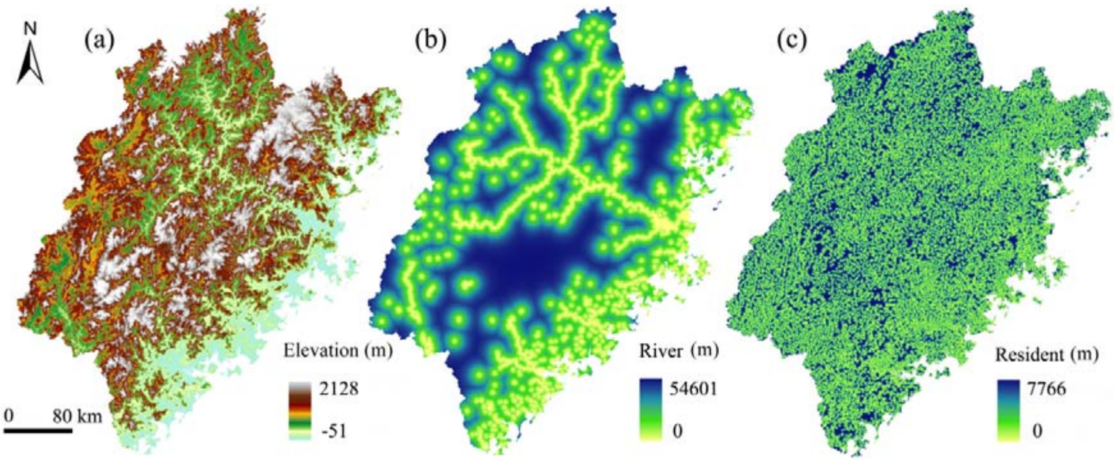

Figure 2 Distribution map of elevation (a), distance to nearest big river (b) or resident (c)

where d_{ij} is the Euclidean distance between regression point i and neighboring observation j, and b represents a basal width of the kernel function, called bandwidth.

A stationarity index was proposed by Brunsdon et al and Osborne et al (Brunsdon et al. 1998; Osborne et al. 2007). It is designed to measure the spatial non-stationarity, and values smaller than 1 indicate stationarity. To calculate the stationarity index, firstly the interquartile range of standard error for GWR coefficients for each explanatory variable were calculated; then twice the standard error of global regression coefficient was also obtained; finally the stationarity index was calculated as the ratio of these two factors.

All candidate variables were firstly normalized by subtracting the mean and dividing by the standard variance. Then the OLS and GWR analysis was carried out using ESRI ArcGIS 9.3 software. The stationary index was calculated using Matlab R2008b based on the method proposed by Brunsdon et al and Osborne et al (Brunsdon et al. 1998; Osborne et al. 2007).

2 Results and Discussions

2.1 Results of global model

An ordinary linear ordinary least square (OLS) regression was firstly carried out (Table 2 and Table 3). The variance inflation factor (VIF) measures the redundancy among explanatory variables. As a rule of thumb, explanatory variables associated with VIF values larger than 7.5 should be removed (one by one) from the regression model. The VIF of all candidate variables selected are smaller than 7.5, and thus are kept in the regression model. Approximately 13.34% or 7.17% of the variation of $EVI_{\max}$ and ΔEVI could be explained respectively. For $EVI_{\max}$, all variables except aspect, distance to road, were statistically significant at the 95% confidence level according to their t-probabilities (Table 2). In particular, elevation, slope, distance to river, proportion of coniferous forest or hardwood forest, had positive correlation with maximum EVI, whereas distance to lake and resident were negatively correlated with maximum EVI. Conditions such as away from big river, close to sub-rivers or lakes might be good condition for vegetation growth, since cities and human activities are dominant near big rivers and also sub-rivers can guarantee the water supply. Both proportion of coniferous forest and hardwood forest had strong positive relationships with $EVI_{\max}$, indicating the good state of forest vegetation.

For ΔEVI, parameters of elevation, distance to nearest big river, road and resident, were statistically significant at the 95% confidence level according to their t-probabilities (Table 3). Particularly, the most important variable was elevation, with the t-values of 96.72. Variables of

Table 1 OLS model parameters estimate for $EVI_{\max}$

Parameters	Coefficient	Standard variance	t-Statistic	p-value	VIF
Intercept	0.4966	0.0002	3,099.9248	0.000000*	-------
Elevation	4.09045	0.0607	67.3947	0.000000*	1.5261
Slope	0.0389	0.0018	21.8797	0.000000*	1.2982
Lake	-4.6666	0.0974	-47.9135	0.000000*	1.0693
River	31.5103	1.5244	20.6708	0.000000*	1.2622
Resident	-0.4732	0.1083	-4.3675	0.000016*	1.1416
Conifer	0.0063	0.0001	62.7651	0.000000*	2.0727
Hardwood	0.0066	0.00009	71.7313	0.000000*	2.0681

Table 2 OLS model parameters estimate for ΔEVI

Parameters	Coefficient	Standard variance	t-Statistic	Probability	VIF
Intercept	0.2386	0.0001	2135.2154	0.000000*	-------
Elevation	3.8747	0.0401	96.7231	0.000000*	1.3649
River	9.4176	1.0614	18.8727	0.000000*	1.2505
Road	-0.2918	0.0809	-3.6034	0.000329*	1.1364
Resident	-0.4715	0.0765	-6.1650	0.000000*	1.1681

elevation and distance to nearest big river have positively correlation with ΔEVI, the amplitude of EVI. Other accessibility variables like distance to the nearest road or resident had negative relationship with ΔEVI. It was suggested that conditions such as high altitude, away from big river and proximate to road or resident might be a good indication for large amplitude of EVI. Results from OLS indicated that for the estimation of both maximum EVI and magnitude of phenological cycles, parameters of elevation, distance to nearest big river and distance to nearest resident are significant.

2.2 Results of GWR model

Detailed statistics for GWR were given in Tables 4 and 5. A parameter or variable is assumed to be non-stationary when inter-quartile range (IQR) of local estimates is greater than ± standard deviation of the equivalent global parameter (Fotheringham et al. 2002). Results demonstrated that all the IQR of estimated parameters by GWR fell outside the ± standard derivation of equivalent OLS parameters. By taking into consideration of the spatial variation of local terrain and accessible condition, the GWR model produced much better fit for the regression relationship between both EVI_{max} and ΔEVI (Table 6). The residual squares for the GWR model are significantly decreased. The percentage of explanation power increased from around ten percent in the global OLS model to 48.05% and 40.89% in GWR for EVI_{max} and ΔEVI respectively. The F test indicated an improvement of GWR over its corresponding OLS. Furthermore, the smaller values of AIC in GWR model also suggested that the GWR model was better as regards to the degrees of freedom. The difference in AIC values between OLS and GWR models was more than 3, indicating the significant difference between those two models. It was evident that the relationship between maximum EVI, magnitude of vegetation phenology and environmental variables including elevation and accessibility is non-stationary across the study area.

For EVI_{max}, OLS estimates for the parameters

Table 3 GWR parameters estimate for EVI_{max}

Parameter	Minimum	25% quartile	Medium	75% quartile	Maximum	Stationary index
Elevation	-224.6222	-0.2710	1.7920	6.1163	366.7458	42.8
Slope	-1.9722	-0.0134	0.0031	0.0300	1.1048	10.6
Lake	-50.3174	-3.4304	-1.6515	0.5638	19.7340	17.7
River	-3,708.2417	-48.5286	38.6327	254.1584	4,789.2115	91.1
Resident	-63.3898	-1.8592	-0.3490	2.2478	68.8025	16.5
Conifer	-0.0634	-0.0012	0.00004	0.0025	0.0651	15.0
Hardwood	-0.0662	-0.0008	0.0005	0.0030	0.0459	15.5

Table 4 GWR parameters estimate for ΔEVI

Parameter	Minimum	25% quartile	Medium	75% quartile	Maximum	Stationary index
Elevation	-107.4475	1.4068	3.5761	5.6455	194.6019	47.2
River	-3,763.2947	-68.8917	26.0122	140.1368	2,389.2651	95.7
Road	-55.7904	-1.4445	0.3644	2.1944	45.0797	22.6
Resident	-32.0359	-2.2576	-0.5267	1.3061	87.8847	22.5

Table 5 Diagnostic information of GWR model for EVI_{max} and ΔEVI

Parameter	EVI_{max}		ΔEVI	
	OLS	GWR	OLS	GWR
Residual Squares	603.2565	245.9132	293.8255	166.3309
AIC	-417,649	-506,151	-524,776	-580,838
R^2	0.1335	0.5139	0.0718	0.4319
Adjusted R^2	0.1334	0.4805	0.0717	0.4089
DF	153,430	153,430	153,433	153,433
F--Statistic	3,376	15,635	2,845	73,312

of proportion of coniferous or hardwood forest were approximately within the 75% quartile and maximum range, and OLS estimates for elevation, slope, were approximately within medium and 75% quartile range, indicating that most local estimates of these parameters are lower than OLS values. Whereas, OLS estimates for parameters of distance to nearest lake were roughly within the minimum and 25% quartile range, and parameters of other accessibility variable including distance to nearest big river or resident, were around 25% quartile range and medium range, revealing that most local estimates of these parameters were higher than OLS values.

For ΔEVI , only OLS estimates for the parameter of elevation were approximately within the medium quartile and 75% quartile range, illustrating higher local estimates of GWR than OLS model (Table 5). OLS estimates of other parameters like distance to nearest big river, road or resident, were approximately within the 25% quartile and medium range, indicating a lower local estimates of GWR than OLS model.

The local values of parameters estimates from GWR can be mapped. The shaded maps of local estimates for three important variables, elevation, distances to nearest big river and to nearest resident, were shown in Figure 3. Those maps of local estimates further highlighted that the association between elevation and accessibility with both $EVI_{\max}$ and ΔEVI varied dramatically across the study area. The map of local estimate of elevation presented increased influence on $EVI_{\max}$ in the southwest, eastern coastal and central north portion but slightly weak and negative effect in several scattered and small central portions. Another map of local estimate of elevation indicated nearly universal positive effect on $EVI_{\max}$ with negative influence on few localized areas in the southeast portion near the coast. Similarly, the map of local estimate of distance to nearest big rivers suggested a very strong positive influence on both $EVI_{\max}$ and ΔEVI within areas near those big rivers and coastal areas. It seemed that the map of distance to nearest resident suggested no obvious distribution trend across the space, with both negative and positive influence scattered on the whole image. But if we compared it with the spatial distribution map of distance to resident, we could find that very positive influence

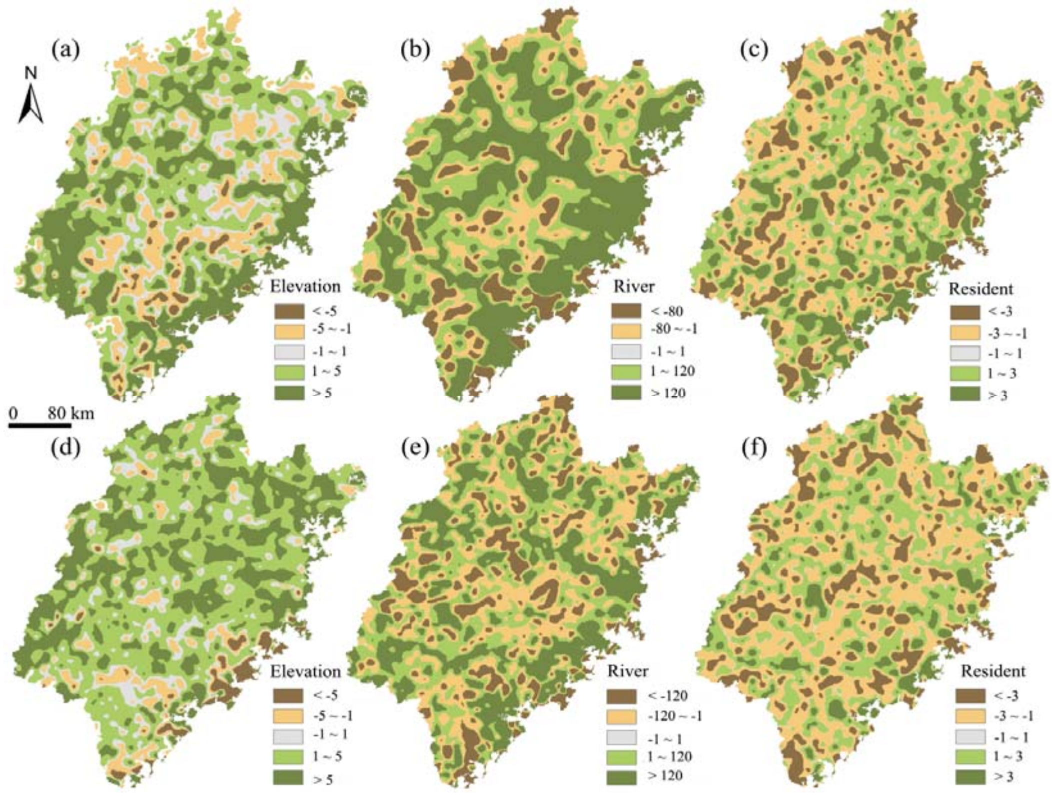

Figure 2 Spatial distribution of GWR estimates for coefficient of elevation, distance to nearest big river or resident for $EVI_{\max}$ ((a), (b), (c); coefficient of elevation, distance to nearest big river or resident for ΔEVI ((e), (f), (g))

on both $EVI_{\max}$ and ΔEVI were within those areas close to nearest residents and negative effect were far away from them. Their local estimate values were among the range of -63~75, -33~42 for $EVI_{\max}$ and ΔEVI respectively.

2.3 Altitudinal variation in the EVI-elevation relationship

The local values of the parameters estimates provides the information about the spatial variability of the $EVI_{\max}$ -altitudinal relationship. To analyze the effect of terrain elevation on the local estimates, we examines mean value of the original $EVI_{\max}$ and its local estimate in the following latitudinal bands: below 100 m, 100 m-200 m, 200 m-400 m, 400 m-600 m, 600 m-800 m, 800 m-1,000 m, 1,000 m-1,200 m, 1,200 m-1,300 m, 1,300 m-1,500 m and above 1,500 m. Results demonstrate that substantial altitudinal variations in both the original $EVI_{\max}$ and its local estimate (Figure 4a).

The local estimates of $EVI_{\max}$ -altitudinal coefficient generally decreases with the altitude (Figure 4a). It varied dramatically from strong positive to slightly negative values with increasing altitude. Its mean value was 17.48 for the lowest altitudinal band of below 100 m and -0.86 for the altitudinal band of above 1,500 m. The value of local estimate of EVI-altitudinal relationship was strongly positive for the altitude band of below 100 m, indicating marvelous increase of EVI with increasing elevation above sea level. The rate of increase of EVI with elevation gradually drops at the altitudinal range from 100 m to 1,200 m. The local estimates changed to a negative value within

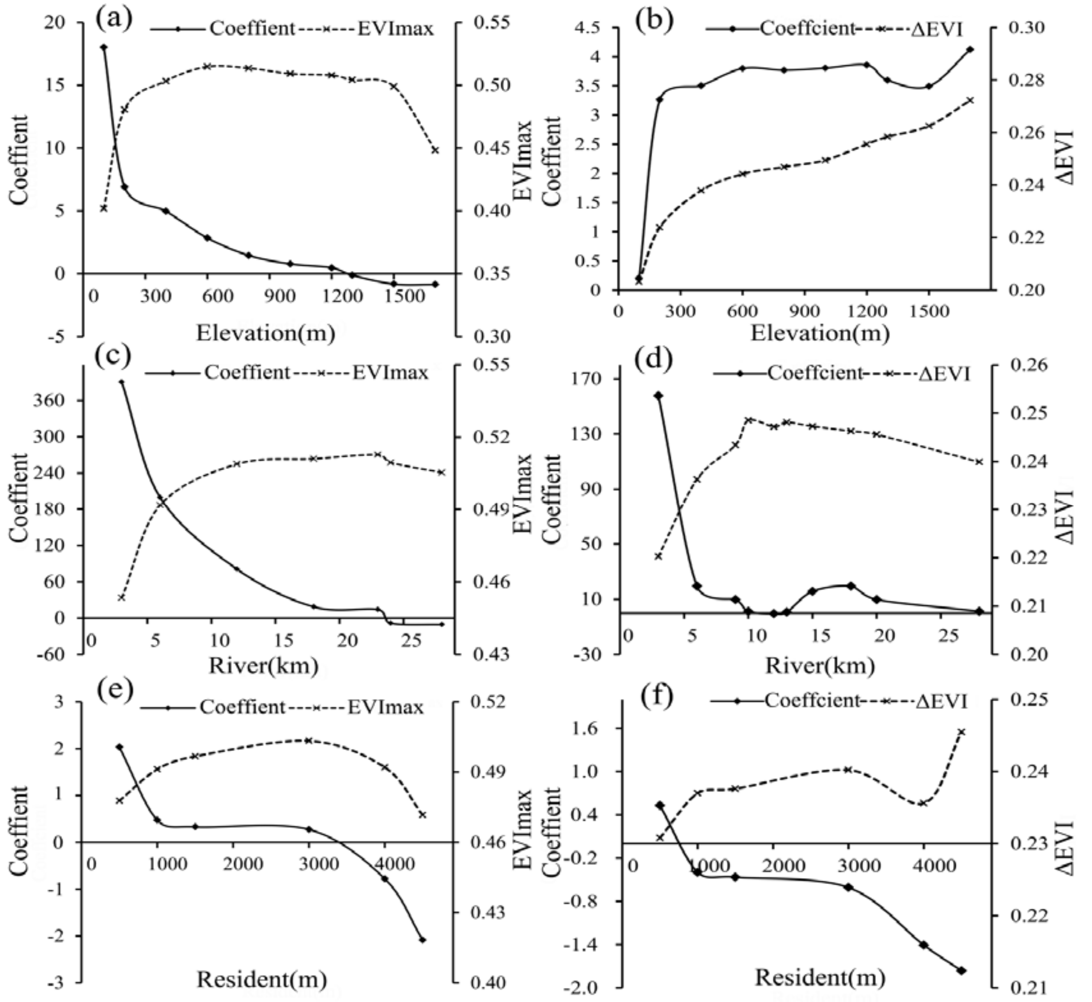

Figure 3 Variations in the coefficient of elevation with (a) $EVI_{\max}$, (b) ΔEVI , distance to nearest big river with (c) $EVI_{\max}$, (d) ΔEVI , distance to resident with (e) $EVI_{\max}$, (f) ΔEVI

the next altitudinal band (1,200 m-1,300 m). For altitudinal bands above 1,200 m, the value of its local estimates for EVI-altitudinal relationship was negative, suggesting a decrease trend of EVI with increasing altitude.

EVI or NDVI of vegetation generally presented a complex relationship along the altitudinal transects, probably as a result of a complicated trend of climate factors with increasing elevation (Xie and Liu 2010). The amount of precipitation and available solar energy generally increase with altitude, but only to a certain altitude. Beyond this level, both the amount of precipitation and the solar energy may drop. Furthermore, the temperature may decrease along with the increasing elevation. The composition of variation in these important climate factors adds the complexity of vegetation-altitude relationship. According to the results of this study, the combination of environmental factors seemed to be the most appropriate at around 600 m -1,000 m. The average $EVI_{\max}$ located within the altitudinal band of 600 m -1,200 m showed the greatest values (Figure 4a). $EVI_{\max}$ generally decreased when below or above this altitudinal range. Results from this study showed that a significant increase of EVI was observed from 0-400 m, and a subsequent decrease of EVI above 1,200 m. Thus the GWR model provided abundant information on the elevation-$EVI_{\max}$ relationship across the space and different altitude bands, whereas only the positive correlation could be observed from the OLS model.

Similarly, local values of the parameter estimates provide the information about the spatial variability of the ΔEVI -altitudinal relationship. The effect of elevation on its local estimates was also examined. Substantial altitudinal variations in both the original ΔEVI and its local estimate were shown in Figure 3b. Generally, the local estimates of coefficient (ΔEVI -elevation) increased with altitude, especially in the range of below 200 m. In the altitudinal range of 200 m-1,500 m, very strong positive correlation of ΔEVI -elevation was observed, indicating a remarkable magnitude of phenological cycle with altitude. Little variation was observed in the correlation of ΔEVI -elevation in this range. Above 1,500 m, significantly increase was discovered in the coefficient of ΔEVI -elevation. Its mean value was 17.48 for the lowest altitudinal band of below 100 m and -0.86 for the altitudinal band of above 1,500 m.

Research on phenology could be dated back to several decades (Allen and Breshears 1998). Most related research focused on the onset, offset dates of vegetation phenology cycles and its variation as a result of climate change (Ahas et al. 2002; Sobrino et al. 2011). Very little attention is drawn on the magnitude of its phenology cycles and its possible reasons. This study reveals that the magnitude of vegetation phenology increase with altitudinal gradient, and the increase extent depends on specific altitudinal transects. In the altitudinal range of below 100 m, land surface was occupied by human activities, primarily by cities, town, agricultural crops and vegetables, and water body, with low EVI value and magnitude phenology cycles. Economic forest was dominant in the altitudinal range of 100 m-200 m, with slightly weak EVI value and magnitude phenology cycles. According to the results of this study, there was no distinct difference between hardwood and coniferous forest as regards to its growth state and phenology cycles in subtropical areas. Above 1,500 m, meadow and small pine trees cover these area, with much lower growth state and stronger phenology cycles. Patterns of both $EVI_{\max}$ -altitudinal and ΔEVI -altitudinal relationship are very complicated, due to the combination of environmental factors, vegetation composition and anthropogenic impact.

2.4 Accessible variation in the EVI-accessibility relationship

The local values of the parameter estimates provided the information about the spatial variability of the EVI-accessibility relationship. To analyze the effect of accessibility on the local estimates, we examined the mean value of the original $EVI_{\max}$ and its local estimate in the following bands for parameter of distance to nearest big river: 0-3 km, 3 km-6 km, 6 km-9 km, 9 km-10 km, 10 km-12 km, 12 km-13 km, 13 km-15 km, 15 km-18 km, 18 km-20 km and above 20 km. Results demonstrated that substantial altitudinal variations in both the original $EVI_{\max}$ and its local estimate (Figure 3c).

Exactly conformed to the $EVI_{\max}$ -altitudinal relationship, the $EVI_{\max}$ -river coefficient displayed substantial decrease with increasing distance to nearest big rivers (Figure 3c). It changed dramatically from strong positive to slightly negative values with increasing altitude. The value of local estimate of EVI_{max} -river relationship was strongly positive for the altitude band of 0-6 km, indicating great increase in EVI with increasing distance to nearest big rivers. The rate of increase of EVI with distance to nearest big rivers gradually dropped as the altitude increase from 6km to 12km. The local estimates changed to negative values with a distance of more than 23 km away from the nearest big rivers, suggesting a slightly decrease trend in EVI with increasing distance from the big rivers.

Also conformed to the EVI_{max} -river relationship, dramatic decrease was observed from the ΔEVI -river relationship with increasing distance to nearest big rivers, especially below 6km (Figure 3d). When the distance to nearest river was above 6 km, the value and variation of relationship was fairly small except a gentle increase in the range of 13 km-18 km.

It was interesting that the dynamic of EVI_{max} and ΔEVI values along with distance to nearest big river were comparable, both showing a dramatic increasing trend and steady level after a certain distance. Within the distance of 10 km -12 km, both EVI_{max} and ΔEVI obtained the peak values. Both indices indicated no obvious trend with the distance of above 12 km to nearest big river (Figure 3c, Figure 3d). In Fujian province, areas within 6 km from big river were generally occupied by cities or towns and crops, with generally weak EVI_{max} and ΔEVI values. Very strong positive relationship was observed within that area, due to the increase of vegetation along with distance to big rivers. Areas with distance of over 12 km to nearest big river were almost completely covered by forests, thus there was no obvious strong relationship with variable of distances to big river with both EVI_{max} and ΔEVI within this area.

Similarly, the effect of another accessibility variable, distance to nearest resident, on its local estimates was also evaluated. We calculated the mean value of the original EVI_{max} and its local estimate in the following bands for parameter of distance to nearest resident: 0-0.5 km, 0.5 km-1 km, 1 km-1.5 km, 1.5 km-3 km, 3 km-4 km and above 4 km. Substantial altitudinal variations in both the original EVI_{max} , ΔEVI and its local estimate were shown in Figure 3e, Figure 3d, respectively. When the distance to nearest resident increased from 0km to 1 km, the coefficient of EVI_{max} -resident, ΔEVI -resident decreased significantly. While the distance to nearest resident was within the range of 1 km-3 km, there was little variation in their relationship. Within areas with the distance to nearest resident above 4 km, the elevation was generally above 1,000 m. The spatial pattern of their relationship within those areas was controlled by elevation. Thus it was not strange that almost exactly the same spatial distribution patterns were observed from both EVI_{max} -resident and ΔEVI -resident relationship with elevation in the study area.

3 Conclusion

This study investigated the influence of topography and accessibility on the annual maximum EVI and phenological magnitude in a region with diverse terrain conditions in Fujian, China, using GWR models based on the multiple time scale decomposition of MODIS EVI time series datasets through wavelet transform. It was revealed that parameters of elevation, accessibility to nearest big river and resident, had significantly influence on both maximum EVI and phenological magnitude. Results from OLS showed that ranking as the most important parameter, altitude had very strong positive effect on maximum EVI and phenological magnitude. Similarly, variable of accessibility to nearest big river also had positive influence on them. Conversely, variable of accessibility to nearest resident had negative relationship with both maximum EVI and phenological magnitude. GWR analysis indicated that spatially, the parameters of topography and accessibility might had strong or weak, positive or negative influence on both maximum EVI and phenological magnitude on different regions of Fujian province, characterized by cracked topography with mountains, hills and rivers. For example, the relationship of EVI-altitude changed from strongly positive in regions at altitude below 200 m to slightly negative in regions above 1,500 m. Instead of the mono negative influence of accessibility to nearest resident on maximum EVI and phenological magnitude derived from OLS results, positive relationship was also observed within a certain distance from GWR results. In terms of the magnitude of the altitudinal gradient, the most rapid change of maximum EVI was observed below 200 m, and the most rapid change of phenological magnitude was discovered above 200 m, especially above 1,500 m. Regarding the magnitude of the accessible gradient, the most dramatic changes of maximum EVI and phenological magnitude were discovered within distance to nearest big river below 3 km. It seemed that the most rapid change of coefficient between maximum EVI & phenological magnitude and topography & accessibility was observed within a low elevation or close distance. Considerably less variation of their relationship was detected within a certain range of medium altitude or distance. However, their relationship might change when above this range. Patterns of topography and accessibility had a very complex influence on both maximum EVI and phenology magnitude, as a result of the various combinations of environmental factors, vegetation composition and also anthropogenic impact.

This study demonstrated that the non-stationary analysis of wavelet transform smoothed time-series vegetation index through the framework of GWR could lead to a better understanding of both vegetation distribution and its phenology cycles in subtropical mountainous and hilly region.

Acknowledgement

The authors would like to thank NASA LP DAAC for making MODIS data available. We gratefully acknowledge the financial support for this work from Chinese National Natural Science Foundation (Grant no. 41071267), Scientific Research Foundation for Returned Scholars, Ministry of Education of China ([2012]940) and Science Foundation of Fujian province (Grant no. 2012J01167, 2012I0005).We are also grateful to the anonymous reviewers for offering valuable suggestions to improve the manuscript.

Reference

Abry P (1997) Ondelettes et turbulence. In: Diderot (Ed.) Multiresolutions, algorithmes de decomposition, invariance dechelles. Paris. p 268.

Ahas R, Aasa A, Menzel A, et al. (2002) Changes in European spring phenology. International Journal of Climatology 22(14):1727-1738.

Allen CD, Breshears DD (1998) Drought-induced shift of a forest-woodland ecotone: rapid landscape response to climate variation. Proceedings of the National Academy of Sciences 95(25): 14839-14842.

Atzberger C, Eilers PHC (2011) A time series for monitoring vegetation activity and phenology at 10-daily time steps covering large parts of South America. International Journal of Digital Earth 4(5):365-386.

Beatriz Martínez, Gilabert MA (2009) Vegetation dynamics from NDVI time series analysis using the wavelet transform. Remote Sensing of Environment 113(9):1823-1842.

Ben - Ze'ev E, Karnieli A, Agam N, et al. (2006) Assessing vegetation condition in the presence of biomass burning smoke by applying the Aerosol-free Vegetation Index (AFRI) on MODIS images. International Journal of Remote Sensing 27(15):3203-3221.

Brunsdon C, Fotheringham AS, Charlton ME (1998) Geographically weighted regression - modelling spatial non-stationarity. The Statistician 47(3):431-443.

Chamaille–Jammes S, Fritza H, Murindagomoc F (2006) Spatial patterns of the NDVI–rainfall relationship at the seasonal and interannual time scales in an African savanna. International Journal of Remote Sensing 27 (23):5185-5200.

Chang CT, Lin TC, Wang SF, et al. (2011) Assessing growing season beginning and end dates and their relation to climate in Taiwan using satellite data. International Journal of Remote Sensing 32(18):5035-5058.

Crimmins TM, Crimmins MA, David Bertelsen C (2010) Complex responses to climate drivers in onset of spring flowering across a semiarid elevation gradient. Journal of Ecology 98(5):1042-1051.

Fotheringham AS, Brunsdon C, Charlton M (2002) Geographically weighted regression: the analysis of spatially varying relationships. In. John Wiley & Sons Inc, Chichester.

Fujian Tpsgo (2010) Fujian Yearbook. Fujian People's Publishing House, Fuzhou, China.

Foody GM (2003) Geographical weighting as a further refinement to regression modelling: An example focused on the NDVI-rainfall relationship. Remote Sensing of Environment 88(3):283-293.

Gao Y, Huang J, Li S, et al. (2012) Spatial pattern of non-stationarity and scale-dependent relationships between NDVI and climatic factors- a case study in Qinghai-Tibet Plateau, China. Ecological Indicators 20:170-176.

Gao ZW (2004) Research on forest resource management. Fujian Cartographic Publisher, Fuzhou, China.

Huete A, Didan K, Miura T, et al. (2002) Overview of the radiometric and biophysical performance of the MODIS vegetation indices. Remote Sensing of Environment 83(1-2):195-213.

Iversen M, Bråthen KA, Yoccoz NG, et al. (2009) Predictors of plant phenology in a diverse high-latitude alpine landscape: growth forms and topography. Journal of Vegetation Science 20(5):903-915.

Justice CO, Vermote E, Townshend JRG, et al. (1998) The Moderate Resolution Imaging Spectroradiometer (MODIS): Land remote sensing for global change research. IEEE Transactions on Geoscience and Remote Sensing 36(4):1228-1249.

Li A, Deng W, Liang S, et al. (2010) Investigation on the

patterns of global vegetation change using a Satellite-Sensed Vegetation Index. Remote Sensing 2(6):1530-1548.
Liang S, Ge S, Wan L, et al. (2012) Characteristics and causes of vegetation variation in the source regions of the Yellow River, China. International Journal of Remote Sensing 33(5):1529-1542.
Lu SJ (1999) Fujian Climate. China Meteorological Press, Beijin, China.
Martínez B, Gilabert MA (2009) Vegetation dynamics from NDVI time series analysis using the wavelet transform. Remote Sensing of Environment 113(9):1823-1842.
Moulin S, Kergoat L, Viovy N, et al. (1997) Global-Scale Assessment of Vegetation Phenology Using NOAA/AVHRR Satellite Measurements. Journal of Climate 10 (6):1154-1170.
Nelson A, Oberthür T, Cook S (2007) Multi-scale correlations between topography and vegetation in a hillside catchment of Honduras. International Journal of Geographical Information Science 21 (2):145-174.
Ogden J, Powell JA (1979) A quantitative description of the forest vegetation on an altitudinal gradient in the Mount Field National Park, Tasmania, and a discussion of its history and dynamics. Australian Journal of Ecology 4(3):293-325.
Osborne PE, Foody GM, Suárez-Seoane S (2007) non-stationarity and local approaches to modeling the distribution of wildlife. Diversity and Distributions 13(3):313-323.
Pagano TS, Durham RM (1993) Moderate resolution imaging spectroradiometer (MODIS). Proc. SPIE 1939, Sensor Systems for the Early Earth Observing System Platforms. p2. DOI: 10.1117/12.152835.
Piao SL, Cui M, Chen A, et al. (2012) Altitude and temperature dependence of change in the spring vegetation green-up date from 1982 to 2006 in the Qinghai-Xizang Plateau. Agricultural and Forest Meteorology 151(12):1599-1608.
Piao SL, Mohammat A, Fang J, et al. (2006) NDVI-based increase in growth of temperate grasslands and its responses to climate changes in China. Global Environmental Change 16(4):340-348.
Pineda Jaimes NB, Sendra JB, et al. (2010) Exploring the driving forces behind deforestation in the state of Mexico (Mexico) using geographically weighted regression. Applied Geography 30(4):576-591.
Propastin P (2011) Multiscale analysis of the relationship between topography and aboveground biomass in the tropical rainforests of Sulawesi, Indonesia. International Journal of Geographical Information Science 25 (3):455-472.
Propastin P (2012) Modifying geographically weighted regression for estimating aboveground biomass in tropical rainforests by multispectral remote sensing data. International Journal of Applied Earth Observation and Geoinformation 18:82-90.
Rowhani P, Linderman M, Lambin EF (2011) Global interannual variability in terrestrial ecosystems: sources and spatial distribution using MODIS-derived vegetation indices, social and biophysical factors. International Journal of Remote Sensing 32(19):5393-5411.
Sobrino JA, Julien Y, Morales L (2011) Changes in vegetation spring dates in the second half of the twentieth century. International Journal of Remote Sensing 32(18):5247-5265.
Souza AA, Galvao LS, Santos JR (2010) Relationships between Hyperion-derived vegetation indices, biophysical parameters, and elevation data in a Brazilian savannah environment. Remote Sensing Letters 1(1):55-64.
Wang JF, Liu X, Christakos G, et al. (2010) Assessing local determinants of neural tube defects in the Heshun Region, Shanxi Province, China. BMC public health 10(1):52.
Waring RH, Coops NC, Fan W, et al. (2006) MODIS enhanced vegetation index predicts tree species richness across forested ecoregions in the contiguous USA. Remote Sensing of Environment 103(2):218-226.
Xie J, Liu T (2010) Characterization of spatial scaling relationships between vegetation pattern and topography at different directions in Gurbantunggut desert, China. Ecological Complexity 7(2):234-242.
Zhao N, Yang Y, Zhou X (2010) Application of geographically weighted regression in estimating the effect of climate and site conditions on vegetation distribution in Haihe Catchment, China. Plant Ecology 209(2):349-359.
Zhong L, Ma Y, Salama M, et al. (2010) Assessment of vegetation dynamics and their response to variations in precipitation and temperature in the Tibetan Plateau. Climatic Change 103(3):519-535.